

LETTER

OPEN

ANIMAL MODELS

asxl1 C-terminal truncation and SRSF2 mutation drive leukemogenesis via immune reprogramming

Lingge Tu¹, Fangfang He¹, Jun Mun Liew¹, Chun-Fung Sin², Lichuan Zheng¹, Sze-Pui Tsui², Xinyu Miao¹, Hoi-yi Chan², Alvin Chun Hang Ma^{1,4}, Wenqing Zhang^{1,5,6}, Yiyue Zhang¹, Anskar Y. H. Leung^{1,4,7}✉ and Xuan Sun^{1,4}✉

© The Author(s) 2025

Leukemia (2025) 39:3047–3051; <https://doi.org/10.1038/s41375-025-02790-5>



TO THE EDITOR:

Acute myeloid leukemia (AML) carrying mutations pertinent to chromatin-modification and spliceosome represents an aggressive subtype with poor prognosis. Specifically, mutations of genes encoding additional sex combs-like 1 (ASXL1), a member of the polycomb protein family [1, 2], and serine/arginine-rich splicing factor 2 (SRSF2), a member of RNA splicing machinery [3, 4], are frequently found in myeloid neoplasms [5–7]. The co-occurrence of ASXL1 and SRSF2^{P95H} mutations leads to a significantly worse prognosis than having either mutation alone, indicating a synergistic effect in leukemogenesis [1]. Mice engineered with the Asxl1 C-terminal truncation and the Srsf2^{P95H} mutation developed leukemia characterized by a myeloid-biased hematopoietic stem cell (HSC) pool and a malignant transcriptomic signature [1]. These findings correlate mutation combinations to leukemia progression, but the mechanisms driving leukemogenesis remain unclear, hindering targeted therapy development.

Herein, we developed a zebrafish model carrying both mutations to gain new insights into the mechanisms underpinning the pathogenic synergism between asxl1 and SRSF2^{P95H}. By crossing zebrafish with a C-terminal truncation mutation in asxl1 [8] (referred to as "A") with Tg(Runx1: SRSF2^{P95H}) (referred to as "S") transgenic zebrafish, which expresses the SRSF2^{P95H} mutation under the Runx1 promoter in the HSPC population [9] (Supplementary Fig. 1), we have generated a double mutant zebrafish model (referred to as "SA"). At the embryonic stage, SA embryos showed a significant increase in myeloid progenitors, as shown by pu.1 expression, which was higher than asxl1 deletion or transgenic SRSF2^{P95H} alone (Fig. 1A, E). At 9–12 months, these double mutants exhibited an expanded monocytic compartment in their kidney marrow (KM), compared with the single mutants, as indicated by increased fluoride-sensitive NSE expression (Fig. 1B, F). Additionally, they exhibited higher KM blast

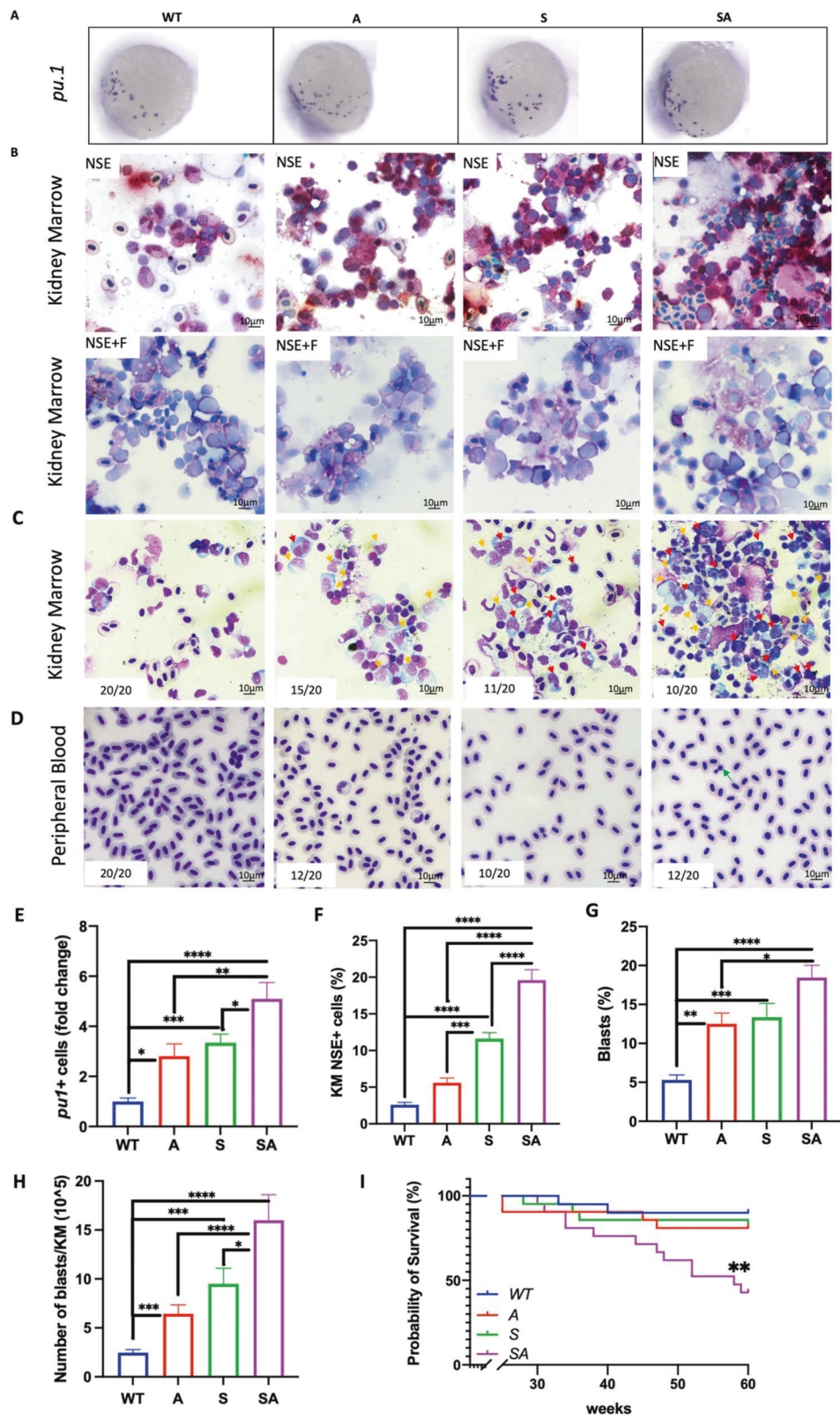
percentages and counts compared to WT and single mutants (Fig. 1C, G, H) and peripheral blood dyserythropoiesis (Fig. 1D). Survival of SA was significantly shorter (Median survival: SA: 42 weeks vs A, S or wildtype: Not reached) (Fig. 1I). These findings corroborated with the observations from the mouse model [1] and reflected the clinicopathologic characteristics of CMML in patients, where these mutations are highly prevalent [5, 6].

The oncogenic potential of SA cells was evaluated by serial transplants. Donor KM cells from WT, A, S and SA zebrafish in Tg(mpo: EGFP) background were transplanted into Casper recipients [10] (Supplementary Fig. 2A). By Day 21 post-transplantation, flow cytometry revealed a trend of increased engraftment in recipients of SA mutant cells (Supplementary Fig. 2B–D), along with increased expression of human SRSF2 in recipients of S or SA mutant cells (Supplementary Fig. 2E). Morphological analysis of the recipient KM revealed progressive disease driven by SA cells. This was characterized by increased blasts, monocytosis, dyserythropoiesis, and reduced myeloid precursors and neutrophils. (Supplementary Fig. 3A–F). Furthermore, serial transplants shortened survival for SA recipients (median survival: 16, 12, and 9.5 days for 1st, 2nd, and 3rd transplants, respectively, vs. WT: not reached), with single mutants showing less pronounced effects (Supplementary Fig. 3G–I). These data suggested that co-existing SRSF2^{P95H} and asxl1 mutations conferred leukemogenic potential in zebrafish that was accentuated upon serial transplants.

To better understand the mechanistic changes induced by SRSF2^{P95H} and asxl1 mutations, RNA sequencing was performed in KM cells from the WT, single, and double mutants. Gene ontology (GO) analysis of the up-regulated differentially expressed genes (DEGs) from SA KM cells revealed significant enrichment in biological processes related to transcriptional regulation and protein ubiquitination (Fig. 2A). Conversely, the down-regulated DEGs were predominantly enriched in pathways associated with

¹Department of Medicine, School of Clinical Medicine, Li Ka Shing Faculty of Medicine, The University of Hong Kong, Pokfulam, Hong Kong. ²Department of Pathology, Queen Mary Hospital, Pokfulam, Hong Kong. ³Department of Health Technology and Informatics, The Hong Kong Polytechnic University, Hung Hom, Hong Kong. ⁴ZeBlast Technology Limited, Ap Li Chau, Hong Kong. ⁵Division of Cell, Developmental and Integrative Biology, School of Medicine, South China University of Technology, Guangzhou, China. ⁶Department of Hematology, Guangzhou First People's Hospital, School of Medicine, South China University of Technology, Guangzhou, China. ⁷Centre for Oncology and Immunology, Hong Kong Science Park, Hong Kong. ✉email: ayhleung@hku.hk; xuansun@hku.hk

Received: 20 May 2025 Revised: 15 September 2025 Accepted: 13 October 2025
Published online: 3 November 2025



neutrophil regulation, protein transport, and immune and inflammatory responses (Fig. 2A). Additionally, Gene set enrichment analysis (GSEA) revealed significant down-regulation of pathways related to immune and inflammatory processes in SA KM cells, further supporting an overall immune-suppressive milieu

in the KM of SA mutant zebrafish (Fig. 2B). To evaluate whether this immune-suppressive phenotype is conserved across species, we analyzed DEGs from *Asxl1*^{Y588X}Tg; *Srsf2*^{P95H/+} mice carrying both mutations [1] and found consistent down-regulation of immune response-related pathways and genes, including the

Fig. 1 Development of chronic myelomonocytic leukemia (CMML) phenotype in *asxl1*^{+/−} and *SRSF2*^{P95H} zebrafish. **A** Representative WISH staining of *pu.1* in embryos from wildtype (WT), *asxl1*^{+/−} (referred to as A), *SRSF2*^{P95H} (referred to as S), and *asxl1*^{+/−} *SRSF2*^{P95H} (referred to as SA). **B** Representative images of NSE staining of WT and mutant kidney marrow (KM) cells. Representative images of NSE with fluoride staining of WT and mutants ($n = 20$ for each genotype). **C** Representative Wright's staining of KM and **D** peripheral blood (PB) smear of the WT and mutants. Blast-like cells in the KM were indicated by red arrows. Monocytes in the KM were indicated by yellow arrows. Dyserythropoiesis in the PB were indicated by green arrows. **E** The percentage of *pu.1* positive cells in WT and mutants ($n = 20$ for each genotype, 9–12 month old fish). **F** The percentage of NSE⁺ cells in the KM of WT and mutants ($n = 20$ for each genotype, 9–12 month old fish). **G** The percentage and **H** the number of blasts in the KM of WT and mutants ($n = 20$ for each genotype, 9–12 month old fish). **I** Overall survival of the WT and mutants ($n = 20$ for each genotype). The numbers in the bottom left-hand corner in (**C**, **D**) indicate the number of fish with the characteristic phenotypes / the total number of fish in each group. One-way ANOVA was performed for (**E–H**), $*P \leq 0.05$, $**P \leq 0.01$, $***P \leq 0.001$, $****P \leq 0.0001$; error bars, mean \pm S.E.M. Log-rank test was performed for (**I**), $**P \leq 0.01$.

immune system process and T cell receptor signaling pathway (Supplementary Fig. 4A, B). Furthermore, comparative analysis of down-regulated DEGs between the double mutant zebrafish and mouse models revealed overlapping suppression of immune response-associated genes, including *Irf7*, *Tnfsf1*, *Rel*, and *Relb* (Supplementary Fig. 4C). The down-regulation of *relb* and *irf7* was further validated in SA mutant zebrafish using qRT-PCR (Supplementary Fig. 4D). These findings demonstrate a conserved immune-suppressive signature driven by the combined effects of *SRSF2*^{P95H} and *asxl1* mutations across species. This immune-suppressive phenotype, driven by concurrent *asxl1* and *SRSF2*^{P95H} mutations, is intriguing given that the *SRSF2* mutation is known to promote inflammation in leukemia [11, 12]. These findings suggest that *asxl1* mutations may alter the pro-inflammatory effects of *SRSF2*, supporting leukemia progression by fostering an immune-suppressive microenvironment [13].

Considering the role of the *SRSF2* mutation in inducing missplicing during leukemia pathogenesis, we used replicate Multivariate Analysis of Transcript Splicing (rMATS) [14] to assess alternative splicing patterns in both WT and mutant cells. Among the five known principal types of alternative splicing, viz. skipped exon (SE), mutually exclusive exons (MXE), alternative 5' splice site (A5SS), alternative 3' splice site (A3SS), and retained intron (RI), SE and MXE were predominant (Supplementary Fig. 5A). Pairwise comparisons with the WT control identified 747 significant differentially spliced genes (DSGs) in SA (FDR ≤ 0.05) (Supplementary Fig. 5A). These DSGs showed substantial enrichment in critical pathways such as the JAK-STAT signaling pathway, inflammatory and immune responses, the spliceosome complex, and processes related to leukemogenesis (Supplementary Fig. 5B). Aberrantly spliced transcripts of immune-related DSGs, such as *il15ra* and *il2rgb*, were validated in KM cells using qRT-PCR (Supplementary Fig. 5C, D). Primers flanking the target exon amplified isoforms representing exon inclusion or skipping. Sashimi plot analysis showed similar exon skipping levels for *il15ra* between WT and mutant samples, while *il2rgb* mutants exhibited higher exon inclusion, confirmed by qRT-PCR. However, whether these differences in transcript levels contribute directly to functional changes or are a consequence of broader splicing dysregulation remains to be determined. Furthermore, analysis of overlapping DSGs between SA zebrafish and *Asxl1*^{Y588X}Tg; *Srsf2*^{P95H/+} mice [1], revealed consistent enrichment in metabolic processes and immune-related pathways (Supplementary Fig. 5E). These findings underscore the profound impacts of aberrant splicing on altering molecular functions associated with signaling, immune response, and metabolism in both zebrafish and mice carrying *Asxl1* and *Srsf2* mutations, suggesting these changes are likely of pathological relevance.

Single-cell RNA sequencing was performed to further delineate the cellular changes upon mutation expression. Twenty distinct cell clusters were identified, as defined by respective gene expression profiles (Fig. 2C, Supplementary Fig. 6). In the SA KM cells, there was a notable increase in the population of

HSCs and hematopoietic stem and progenitor cells (HSPC-MPP), indicating a shift towards stemness, which is associated with disease aggression in leukemia. Additionally, there was an expansion in the lymphoid compartments, suggesting a potential alteration in lymphoid lineage commitment. Conversely, the progenitor and mature populations within the myeloid and erythroid compartments were reduced, suggesting underlying disruption of myeloid and erythroid differentiation (Fig. 2C, D).

Gene set variation analysis (GSVA) showed negative enrichment of pathways associated with immune and inflammatory response across most KM cell populations (Fig. 2E). In contrast, the HSC population exhibited pronounced immune activation, characterized by the upregulation of several key inflammation-related genes, including *nkbiaa*, *relb*, *nkfb2*, *irf1b*, *irf7*, *cd40*, *nkfbie*, *nkfb1ab*, *tnfb*, *traf*, *stat1a*, and *nkfb1ab* (Fig. 2E, F). This differential response supports the proposition that co-mutations in *asxl1* and *SRSF2* enhanced inflammatory signaling specifically in HSCs but induced immune-suppression in the neighbouring cells. This dual mechanism may facilitate the expansion of leukemic stem cells by providing a conducive environment for their survival and proliferation while simultaneously dampening immune surveillance against the cancer cells. In this context, animal models have allowed investigations of the molecular and cellular effects of well-defined gene mutations and their combinations. Analysis of primary samples from patients with AML was confounded by the presence of co-existing mutations, chromosomal translocations and clonal diversity. Whether the aforementioned immune reprogramming in the zebrafish and mouse models could be generalized to human diseases would have to be further examined.

Results from the present study are clinically relevant. While *SRSF2* mutations are linked to inflammation and immune activation, the role of *ASXL1* mutations in these processes has been unclear [2, 11]. Using bulk and single-cell RNA-seq, we demonstrated immune activation in HSCs and immune suppression in neighboring cells, bridging this gap. These findings, supported by *in silico* mouse transcriptome analyses, suggest a conserved pathogenetic role for the double mutations. The observed immune-activated HSCs within an immunosuppressive BM milieu offer therapeutic targets against aberrant splicing and immune signaling in leukemic stem cells.

In conclusion, this study demonstrates the synergistic role of *asxl1* and *SRSF2* mutations in promoting leukemogenesis, as shown in zebrafish and supported by mouse and human data [1]. The conserved pathological effects across species highlight zebrafish as a robust model for therapeutic development. Our findings reveal a complex interaction between these mutations, immune modulation, and cellular differentiation, providing a basis for strategies targeting the leukemia-promoting and immunosuppressive microenvironment. Further investigation is needed to elucidate the molecular and protein-level mechanisms underlying these co-mutations in leukemogenesis.

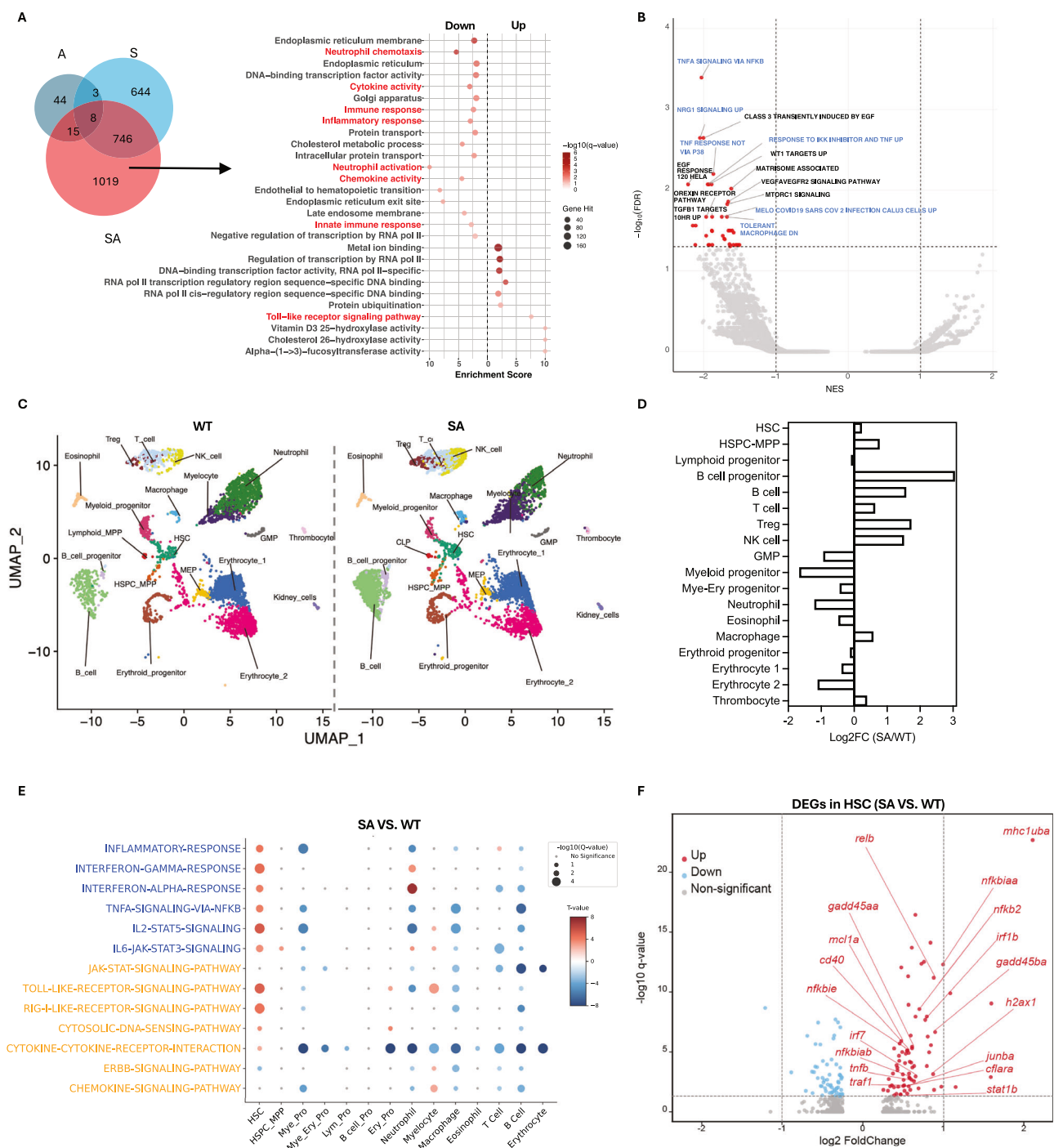


Fig. 2 Concurrent mutations of *asxl1* and *SRSF2* promote leukemogenesis via immune reprogramming in zebrafish. **A** Bulk RNA sequencing was performed using kidney marrow (KM) cells from wildtype (WT), *asxl1*^{+/−} (referred to as A), *SRSF2*^{P95H} (referred to as S), and *asxl1*^{+/−} *SRSF2*^{P95H} (referred to as SA). Venn diagrams of differentially expressed genes (DEGs) among A, S and SA (after compared with WT) (left) and GO-BP enrichment analysis of DEGs of SA double mutants (Right). Immune-related pathways were labelled in red. **B** The volcano plot showed up- or down-regulated gene signatures by GSEA (Hallmark and C2 pathway). The X-axis showed the normalised enrichment score (NES), and the Y-axis showed the corresponding $-\log_{10}$ (FDR). Immune-related pathways were labelled in blue. **C** Single-cell RNA sequencing was performed on kidney marrow (KM) cells from WT and SA zebrafish, followed by Uniform Manifold Approximation and Projection (UMAP) analysis to visualize cell clusters. **D** The log2 fold change (Log2FC) for each cluster in the SA mutant was calculated as the ratio of the number of cells in the SA mutant to the number of cells in the WT for that cluster. **E** Gene Set Variation Analysis (GSVA) was performed to assess enriched immune-related pathway signatures in various hematopoietic cell clusters of SA fish, highlighting immune-related Hallmark pathways (purple) and KEGG pathways (orange). **F** Volcano plot of differentially expressed genes (DEGs) in SA relative to WT HSC, selected genes based on enriched pathways are labelled.

DATA AVAILABILITY

The RNA-Seq data generated in this study have been deposited in the National Center for Biotechnology Information (NCBI) Sequence Read Archive (SRA) under the accession number PRJNA1290872.

REFERENCES

1. Sui P, Ge G, Chen S, Bai J, Rubalcava IP, Yang H, et al. SRSF2 mutation cooperates with ASXL1 truncated alteration to accelerate leukemogenesis. *Leukemia*. 2024;38:408–11.
2. Medina EA, Delma CR, Yang FC. ASXL1/2 mutations and myeloid malignancies. *J Hematol Oncol*. 2022;15:127.
3. Kim WJ, Crosse El, De Neef E, Etxeberria I, Sabio EY, Wang E, et al. Mis-splicing-derived neoantigens and cognate TCRs in splicing factor mutant leukemias. *Cell*. 2025;188:3422–3440.e24.
4. Yoshimi A, Lin KT, Wiseman DH, Rahman MA, Pastore A, Wang B, et al. Coordinated alterations in RNA splicing and epigenetic regulation drive leukemogenesis. *Nature*. 2019;574:273–7.
5. Johnson SM, Richardson DR, Galeotti J, Esperza S, Zhu A, Fedoriw Y, et al. Acute myeloid leukemia with co-mutated ASXL1 and SRSF2 exhibits monocytic differentiation and has a mutational profile overlapping with chronic myelomonocytic leukemia. *Hemisphere*. 2019;3:e292.
6. Marando L, Csizmar CM, Patnail MM. Chronic myelomonocytic leukemia: molecular pathogenesis and therapeutic innovations. *Haematologica*. 2025;110:22–36.
7. Chen TC, Hou HA, Chou WC, Tang JL, Kuo YY, Chen CY, et al. Dynamics of ASXL1 mutation and other associated genetic alterations during disease progression in patients with primary myelodysplastic syndrome. *Blood Cancer J*. 2014;4:e177.
8. Fang X, Xu S, Zhang Y, Xu J, Huang Z, Liu W, et al. Asxl1 C-terminal mutation perturbs neutrophil differentiation in zebrafish. *Leukemia*. 2021;35:2299–310.
9. Wang D, Zheng L, Cheng BYL, Sin CF, Li R, Tsui SP, et al. Transgenic IDH2(R172K) and IDH2(R140Q) zebrafish models recapitulated features of human acute myeloid leukemia. *Oncogene*. 2023;42:1272–81.
10. He F, Tu L, Chan L, Leung A, Sun X. Optimized intravenous injection in adult zebrafish. *J Vis Exp*. 2024. <https://doi.org/10.3791/67463>.
11. McLemore AF, Hou HA, Meyer BS, Lam NB, Ward GA, Aldrich AL, et al. Somatic gene mutations expose cytoplasmic DNA to co-opt the cGAS/STING/NLRP3 axis in myelodysplastic syndromes. *JCI Insight*. 2022;7:e159430.
12. Polleyea DA, Harris C, Rabe JL, Hedin BR, De Arras L, Katz S, et al. Myelodysplastic syndrome-associated spliceosome gene mutations enhance innate immune signaling. *Haematologica*. 2019;104:e388–92.
13. You X, Liu F, Binder M, Vedder A, Lasho T, Wen Z, et al. Asxl1 loss cooperates with oncogenic Nras in mice to reprogram the immune microenvironment and drive leukemic transformation. *Blood*. 2022;139:1066–79.
14. Shen S, Park JW, Lu ZX, Lin L, Henry MD, Wu YN, et al. rMATS: robust and flexible detection of differential alternative splicing from replicate RNA-Seq data. *Proc Natl Acad Sci USA*. 2014;111:E5593–601.

ACKNOWLEDGEMENTS

We thank the Zebrafish Facility from the Centre for Comparative Medicine Research (CCMR) at the University of Hong Kong. We thank Ms Jo Yiu Ling Wong for animal assistance. We thank all participants in the study. We thank OE Biotech Co., Ltd., (Shanghai, China) for providing single-cell RNA-seq and Dr Xiaoying Lu for assistance with bioinformatics analysis. The works were supported by the National Key R & D program of China (2023YFA1800100), Theme-based Research Scheme (T12-702/20-N), Health and Medical Research Fund Projects No.08192066 and No. 08193106, National Natural Science Foundation of China (NSFC)/Research Grants Council (RGC)

Joint Research Scheme 2021/22 N_HKU745/21, 32161160326, the Centre for Oncology and Immunology under the Health@InnoHK Initiative funded by the Innovation and Technology Commission, the Government of Hong Kong SAR, China (AYHL) and Woo Simmy Edith Haematology Research Fund.

AUTHOR CONTRIBUTIONS

LT, AYHL, and XS conceptualised the study and designed the experiments. LT, FH, XS, SPT, HYC, and XM performed the experiments. LT, FH, LZ, and JML performed the bioinformatics analysis. LT, AYHL, and XS analysed the data and wrote the manuscript. CFS, YZ, WQ, and ACM contributed intellectually. All authors approved and contributed to the final version of the manuscript.

COMPETING INTERESTS

The authors declare no competing interests.

ETHICS

The study was approved by the Committee of the Use of Laboratory and Research Animals (CULATR) at the University of Hong Kong (HKU) under approval number CULATR 5649-21. All methods were conducted in accordance with the relevant guidelines and regulations.

ADDITIONAL INFORMATION

Supplementary information The online version contains supplementary material available at <https://doi.org/10.1038/s41375-025-02790-5>.

Correspondence and requests for materials should be addressed to Anskar Y. H. Leung or Xuan Sun.

Reprints and permission information is available at <http://www.nature.com/reprints>

Publisher's note Springer Nature remains neutral with regard to jurisdictional claims in published maps and institutional affiliations.



Open Access This article is licensed under a Creative Commons Attribution-NonCommercial-NoDerivatives 4.0 International License, which permits any non-commercial use, sharing, distribution and reproduction in any medium or format, as long as you give appropriate credit to the original author(s) and the source, provide a link to the Creative Commons licence, and indicate if you modified the licensed material. You do not have permission under this licence to share adapted material derived from this article or parts of it. The images or other third party material in this article are included in the article's Creative Commons licence, unless indicated otherwise in a credit line to the material. If material is not included in the article's Creative Commons licence and your intended use is not permitted by statutory regulation or exceeds the permitted use, you will need to obtain permission directly from the copyright holder. To view a copy of this licence, visit <http://creativecommons.org/licenses/by-nc-nd/4.0/>.

© The Author(s) 2025